AD 712047

Division of Engineering
BROWN UNIVERSITY
PROVIDENCE, R. I.

INELASTIC DEFORMATION OF AN ALUMINUM ALLOY UNDER COMBINED STRESS AT ELEVATED TEMPERATURE

G. M. BROWN

DDC
RECEIVED
SEP 30 1970
B

Department of the Navy
Office of Naval Research
Contract N00014-67-A-0191-0003
Task Order NR 064-424
Technical Report 10

N00014-67-A-0191-0003/10

July 1970

Reproduced by the
CLEARINGHOUSE
for Federal Scientific & Technical
Information Springfield Va. 22151

35

Inelastic Deformation of an Aluminum Alloy Under Combined Stress at Elevated Temperature

by G. M. Brown
Division of Engineering
Brown University
Providence, R. I. 02912

July 1970

Summary

Biaxial stress tests were performed on thin wall tubes of polycrystalline 2024-T81 Aluminum at temperatures of 150 and 250°C. The nominal metallurgical stabilization temperature for this alloy is 190°C. Transient and steady state creep strain rates exhibited a considerable dependence on load path history. For a prescribed history it is possible to determine unique surfaces of constant creep strain rate. For the zero history, involving a single loading from the origin to a prescribed point in stress space, surfaces of constant steady state strain rate, at elevated temperature, have the same shape as room temperature yield surfaces of moderate offset. In the temperature and small strain regions considered here, room temperature yield surfaces were found to be unaffected by elevated temperature deformation. The changes in shape of room temperature yield surfaces, due to room temperature plastic deformation caused corresponding changes in the elevated temperature surfaces of constant steady state creep rate. At a given stress point, an outward local motion of the yield surface resulted in a corresponding outward local motion of the steady state creep rate surfaces. The experimental determination of surfaces of constant flow potential was also attempted.

Technical Report N00014-67-A-0191-0003/10 to the Office of Naval Research

Introduction

The behavior of structural metals under combined stress at room temperature is, in detail, extremely complex. The concepts of a yield surface and the normality relation for plastic strain increments do, however, enable the general characteristics of the material response to be reasonably well understood. At elevated temperature, time effects dominate and the details of material behavior are even more complex. There is no generally accepted elevated temperature equivalent of room temperature phenomenological plasticity theory. The Odqvist Mises-invariant form is often taken as providing a reasonably adequate representation for the secondary creep range of initially isotropic material under constant stress.

This paper presents the results of some fundamental experiments performed on polycrystalline Aluminum in a temperature range in which pronounced time dependent behavior is observed. Emphasis is placed on elucidating the effects of prior combined stressing (loosely phrased, 'history') on material response. The results of several distinct types of test are presented, including:

(1) the history dependence of primary (i.e. transient) creep,

(2) the history dependence of secondary (i.e. steady state) creep,

(3) the interaction of creep and plastic deformation, and

(4) the existence of 'creep surfaces' (DRUCKER 1968, RABOTNOV 1960) and 'flow potential surfaces' (RICE 1970), as analogs of room temperature yield surfaces.

Experimental Method

Combined tension and torsion tests were performed on thin wall tubular specimens of 2024-T81 Aluminum (Fig. 1) at room temperature (23°C) and at 150

and 250°C, (the nominal metallurgical stabilization temperature for this alloy is 190°C). The testing machine has been described previously, FINDLEY & GJELSVIK, (1962) as has the temperature control equipment, BLASS & FINDLEY (1969). In constant load tests, specimen loads were typically held constant to within ±1/20 lb on a 400 lb base load, using a hydraulic loading system, LAI & FINDLEY (1968). Specimen temperatures were held constant within ±0.3°C over a length of 3 1/2", centered on the 2" gauge length, by means of an internal quartz lamp and auxiliary heating cords on either end of the specimen. Specimen strains were measured using an extensometer specifically constructed for this investigation, BROWN (1970a); direct current differential transormers (DCDT's) were used for displacement measurement and in each mode, sensitivity and repeatability were $\sim 2*10^{-6}$ inch/inch while tension-torsion interactions were less than 0.2% (mode 1/mode 2).

Applied loads, specimen deformations and temperature were continuously recorded on strip chart recorders, event markers being used to maintain a common time base. In some tests, a high speed digital data acquisition system was used to obtain a direct digital record of specimen deformations. Strain rates were determined by numerical differentiation of the strain time records; a smoothing technique due to LANCZOS (1964) was used in the calculations in order to reduce the effects of random reading errors.

Experimental Results - Presentation and Discussion

(a) History dependence of primary creep.

One advantage of the continuous recording of specimen deformation is that it is possible to examine the history dependence of transient creep at times very soon after loading has been completed. Figs. 2 and 3 show, respectively, the variations with time of the inelastic strain rate and of the direction of the

instantaneous strain rate vector for the load path shown in the insets to the two figures, at a test temperature of 250°C. For each load increment, the time origin is taken at the instant of cessation of loading (determined from the continuous load-time records). Applied stresses are listed in Table 1 and it may be seen that the load path consists of a large radial step from the origin to a reference stress state, followed by the application and removal of load increments in the radial, tensile and torsional directions. At each load point, the applied loads were changed before the onset of steady state conditions.

The initial direction of the primary strain rate vector is strongly dependent on history (Fig. 3), although an approximately constant value is attained fairly rapidly. The time dependence of the magnitude of the strain rate vector extends over a far greater time, Fig. 2†. The curves obtained after partial loading are all of similar shape, JOHNSON (1951), while those obtained after partial unloading show no corresponding shape similarity.

If a 'creep surface' is defined as the surface orthogonal to the current instantaneous strain rate vector (such surfaces are then equivalent to the flow potential surfaces of RICE (1970), it follows from Figs. 2 and 3 that these instantaneous surfaces exhibit large changes in orientation, particularly in the time range immediately following a change in the applied stress state. The surface normal (here, the inelastic strain rate vector) shows a larger rotation in the case

---

† The second invariant, $\sqrt{\frac{2}{3}\dot{\varepsilon}^p_{ij}\,\dot{\varepsilon}^p_{ij}}$, is used consistently, to determine equivalent strain rates.

of tensile or torsional load increments than for continued radial loading. This result is in agreement with the predictions of a simple polycrystalline model BROWN (1970b).

At corresponding times after loading, curves A and B of Fig. 2 apparently indicate a decreased strain rate with increased load. This phenomenon has been observed by KENNEDY (1963) in uniaxial tests on lead. The test results presented in the next section show that at sufficiently large times the strain rate of load B is larger than that of A.

(b) History dependence of secondary creep.

Relatively few investigations have been performed on the history dependence of steady state creep under biaxial loading and, in general, the tests that have been performed have involved only continued loading. In the selection of experiments whose results are to be used in the development of a suitably general theory, it is necessary to consider cases involving unloading as well as large changes in the direction of the applied stress vector.

Steady state strain rates were determined, at 250°C, at various stress levels along the relatively complex load paths of Fig. 4. In each case, applied loads were held constant until the specimen was well into the steady state. The axial and combined stress levels were the same for all tests, except as noted in Fig. 4. Each test (typically including ~ 8 stress points) was performed on a new specimen.

The magnitudes of the steady state strain rates at the combined stress points of Fig. 4 are shown in Fig. 5. There is, in all cases, an increase in steady state creep strain rates with increasing load point sequence number. This sequence num-

ber provides a qualitative measure of the 'complexity' of the 'load path history'. The increases in strain rate are not due purely to a time-at-temperature effect, since in test 6 the specimen was soaked, at the test temperature of 250°C for 4 hours (approximately half the duration of a typical test sequence), before loading. The increases in strain rate which appear in the earlier tests appear here also, but to a much smaller extent. This difference is attributed primarily to the fact that the load changes in this test were of an incremental magnitude only, and the basic stress state was not changed appreciably.

Variations in the direction of the applied stress vector appear to be an important factor in the determination of the effect of path history on steady state strain rate. In test 4, points 4·1, 4·2, 4·4 and 4·5 were all at the same equivalent stress† and for this test there is still a large change in steady state strain rate with increasing 'load path history', as in the other tests of this set.

(c) Initial secondary creep surfaces.

The results presented in the previous subsection indicate that 'initial' steady state creep rates (i.e. strain rates attained in the steady state following a simple loading from the zero stress state) are fairly reproducible, while the steady state strain rates attained after subsequent loading are strongly dependent on the load path history. For this reason, the following discussion is restricted to 'initial' surfaces of constant steady state creep rate.

The specimens which were used, were machined from extruded tubing. The room temperature yield surface (obtained with an inelastic strain offset of

---

† The selection of an equivalent stress definition is discussed in the following subsection, in the consideration of definitions of creep surfaces.

$\sim 30*10^{-6}$ inch/inch, based on the strain invariant $\sqrt{\frac{2}{3}\dot{\epsilon}^p_{ij}\dot{\epsilon}^p_{ij}}$) was quite anisotropic and was found to be closely approximated by the ellipse

$$\Sigma_{eq}^2 = \Sigma^2 + 5.6T^2$$

where Σ_{eq} = equivalent stress

Σ = tensile stress

T = shear stress

Preliminary experiments indicated that the shape of the 'initial' creep surfaces would be closer to that of the room temperature yield surface than to that of a Mises ellipse ($\Sigma_{eq}^2 = \Sigma^2 + 3T^2$). Stress points, chosen to lie on Mises ellipses, close to the torsion axis gave equivalent creep strain rates for greater than those obtained from points, on the same ellipses, close to the tension axis. Stress points were therefore selected on ellipses of the same slope as the room temperature yield surface and specimens were loaded radially from the origin to the selected stress level. A new specimen was used for each data point.

Tests were performed at 150°C and 250°C in order to determine surfaces with nominal equivalent creep strain rates of $100*10^{-6}$ inch/inch/min. and $10\,000*10^{-6}$ inch/inch/min. Stress levels and inelastic strain rate magnitudes and directions for the low rate surface are given in Table 2, and are plotted in Fig. 6 where it may be seen that the shape of the room temperature yield surface provides an excellent approximation to the shape of the elevated temperature 'initial' secondary creep surface. This result is in agreement with the results of ODQVIST (1966) who used an initially isotropic material (which would give a room temperature yield surface similar in slope to a Mises surface) and who found that the elevated

temperature surface also was similar in slope to a Mises ellipse. Similar results were also obtained by STOWELL & GREGORY (1965) although they were not quite so certain of the initial state of their material. A typical set of curves of equivalent strain rate vs time is shown in Fig. 7; these curves are all of similar shape, in agreement with the observations of JOHNSON (1951).

The results of all tests of this type are summarized in Fig. 8 where it may be seen that over a wide range of temperatures and strain rates, the 'initial' steady state strain rate surfaces are of similar shape. These 'initial' creep surfaces may therefore be predicted from a knowledge of the shape of the room temperature yield surface and a uniaxial stress-strain rate relation at elevated temperature. The results of the previous sub-section show that similar conclusions cannot be drawn for loadings more complex than a simple motion from the origin to a point in stress space. Steady state creep is not path-independent.

(d) Interaction of creep and plastic deformation.

Investigations of the microstructural mechanisms of inelastic deformation of Aluminum at elevated temperature, JOHNSON, YOUNG & SCHWOPE (1955), have shown that, in single crystals, deformation occurs primarily as a result of slip on the slip systems which are operative at ambient temperature. Some additional systems may also be operative but in general, the deformation is in the four [110] directions on each of the three (111) planes. Differences between the room and elevated temperature inelastic deformations appear mainly in the nature of the slip, elevated temperature slip appearing to be much finer than the relatively coarse slip which occurs at room temperature, JOHNSON, YOUNG & SCHWOPE (1955).

In the literature, it is commonly assumed that total strains may be written as a sum of elastic, plastic and 'viscous' parts, PERZYNA (1966), implicitly assuming that there is no interaction between the various components. This subsection presents a brief phenomenological investigation of the interaction between inelastic deformations at room and elevated temperature (i.e. between plastic and creep deformations).

The similarity in shape of initial creep and initial yield surfaces has already been discussed. This similarity holds also for creep surfaces determined after the occurrence of room temperature inelastic deformation†, as shown in Fig. 9 where normalized (the same scale factors were used for both tension and torsion normalization) initial and subsequent yield surfaces are plotted, together with creep surfaces determined for the two material states. In each set of curves, there is a shape similarity, indicating a 'complete interaction' between plastic deformation and creep deformation, in that plastic strains cause corresponding changes in both yield and creep surfaces††.

The converse is not valid. Fig. 10 shows data points for yield surfaces obtained for the virgin state and after both small ($\sim 500 * 10^{-6}$ in/in) and large ($\sim 8000 * 10^{-6}$ in/in) torsional creep strains at elevated temperature; symbols are identified in Table 3. Torsional strains were selected since the specimens

---

† As before, a new specimen was used for each creep data point. For the creep curves after torsional prestrain, all tubes were subjected to the same room temperature plastic prestrain prior to the elevated temperature deformation.

---

†† The creep surfaces mentioned here are, of course, those obtained after the plastic deformation which produced the yield surface used for shape comparisons.

had undergone extensive axial deformations during manufacture and it was felt that if elevated temperature deformation would cause any changes in room temperature behavior, the maximum changes would be produced by torsion. From Fig. 10 it can be seen that the scatter between data points obtained from initial specimens does not differ significantly from the scatter between these points and points obtained at room temperature after elevated temperature torsional creep deformation. Similar results were obtained for a test in which creep deformation occurred along a 45° line in Σ - T space.

Over the range of creep strains examined here, there appears to be no interaction between creep and plastic deformations, in that variations in creep strain cause no noticeable change in the yield surface.

(e) Flow potential surfaces.

Many of the results already presented can be explained in terms of a flow potential theory developed by RICE (1970). In this theory, the instantaneous inelastic strain rate, $\dot{E}^p_{ij}$, is given by the partial derivative of the flow potential Ω (a function of stress and functional of current state), with respect to the corresponding stress, Σ_{ij} , i.e.

$$\dot{E}^p_{ij} = \frac{\partial \Omega}{\partial \Sigma_{ij}}$$

In this sub-section, only the experimental determination of flow potential surfaces will be discussed, the reader being referred elsewhere, RICE (1970), BROWN (1970b) for a discussion of the theory and its applications. In the experimental determination of flow potential surfaces at a given state, there

are two conflicting requirements:

(a) stress excursions must be almost instantaneous, and

(b) stress excursions must be sufficiently slow for measurable inelastic strains to occur.

The first requirement avoids inertia effects and ensures that excessive inelastic strains do not occur, while the second ensures that there is some measurable strain for subsequent calculations. The equipment which was used, was limited to strain rates of the order of $12\ 000 * 10^{-6}$ in/in/min and the results presented here were obtained at approximately this maximum rate. Tests were performed at constant strain rate for the tests involving relatively large changes in total strain and at constant stress rate for the tests involving only relatively small changes in total strain.

The results of the large strain change tests are shown in Fig. 11 where points on surfaces of constant flow potential are plotted, together with the direction of the instantaneous inelastic strain rate vector at that point (from the definition of the flow potential, this vector is also the normal to the surface). A surface similar in shape to that of the room temperature yield surface is also plotted in this figure and it may be seen that curves through the points of constant flow potential would have this same shape. These results are in agreement with the predictions of RICE (1970) where it is shown that yield surfaces may be regarded as an extremely close nesting of potential surfaces.

Fig. 12 shows plots of stress vs time and inelastic strain vs time for a stress cycle superimposed on a steady state tensile strain rate of $\sim 100 * 10^{-6}$ in/in/min. The midpoint of the curve of inelastic strain vs time shows a slight deviation from the smooth curve which might be expected. This is due to the fact

that at the maximum stress level there was a slight delay in decreasing the stress; this delay was due to the nature of the test equipment being used. With a time triangular stress-time curve, the inelastic strain would presumably show a smoothly varying tangent.

The variations in macropotential may be calculated as a function of the stress change and are plotted in Fig. 13. In this figure, the final value of Ω is slightly smaller than the initial value, the difference between initial and final values is, however, less than 5% of the maximum value of Ω for the cycle. Greater accuracy (i.e. a smaller discrepancy between initial and final values of Ω) might be obtained with a reduced cycle time, although, since it is not experimentally possible to fix the internal slipped state, the flow potential cannot be expected to return precisely to its original value.

It was not possible to examine more than this limited degree of path independence, with the equipment available. A more complete examination would, of course, require the investigation of variations in flow potential over a closed cycle in stress space.

Conclusions

Transient and steady state creep strain rates have been shown to exhibit a considerable dependence on load path history. In the transient range, large variations in the direction of the strain rate vector may occur after a small change in the applied stress state. In the secondary range, variations in the direction of the strain rate vector, while maintaining an approximately constant equivalent stress, were found to cause changes in the steady state strain rate.

For a prescribed history, it is possible to define unique surfaces of constant creep strain rate. For the zero history, involving a single loading from the origin to a prescribed point in stress space, the surfaces of constant steady state strain rate at elevated temperature have the same shape as the room temperature yield surface.

Room temperature yield surfaces are unaffected by elevated temperature deformations, in the temperature and small strain regions considered here.

The changes in the room temperature yield surface caused by room temperature plastic deformation cause corresponding changes in the elevated temperature surfaces of constant steady state creep rate. At a given stress point, an outward local motion of the yield surface results in a corresponding outward local motion of the steady state creep rate surfaces.

An investigation of macropotential surfaces, over a very limited range, showed their expected path independence.

Acknowledgment

It is a pleasure to acknowledge the guidance of Professor James R. Rice whose assistance and involvement made the completion of this work possible. Acknowledgment is also due to Professor W. N. Findley for the use of a testing machine in his laboratory and to Mr. Ray Reed for his assistance in the performance of the experiments. The support of the Office of Naval Research under contracts NONR 562(20) and N00014-67-A-0191-0003 with Brown University is gratefully acknowledged.

GMB/dwa

References

BLASS, J. J. and FINDLEY, W.N.	1969	Brown Univ. Tech. Report N00014-67-0191-0003/5
BROWN, G. M.	1970a	Rev. Sci. Instr., 41, 3, 387.
	1970b	Ph.D. Thesis, Brown University
FINDLEY, W. N. and GJELSVIK, A.	1962	Proc. ASTM 62, 1103.
JOHNSON, A. E.	1951	Proc. I Mech. E., 432
JOHNSON, R. D., YOUNG, A. P. SCHWOPE, A. D.	1955	NACA TN-3351
KENNEDY, A. J.	1963	Processes of Creep and Fatigue in Metals, J. Wiley & Sons, N.Y.
LAI, J.S.Y. and FINDLEY, W. N.	1968	Trans. Soc. Rheology, 12:2, 259.
LANCZOS, C.	1964	Applied Analysis, Prentice Hall, London.
ODQVIST, F. K. G.	1966	Mathematical Theories of Creep and Creep Rupture, Oxford.
PERZYNA, P.	1966	Advances in Solid Mechanics, v. 9 Academic Press, N. Y.
RICE, J. R.	1970	Trans. ASME (J. Appl. Mech.)-in press.
STOWELL, E. Z. and GREGORY, R. K.	1965	J. Appl. Mech., March, 37.

TABLE 1

Symbol	Tensile Stress (psi)	Torsional Stress (psi)
A	11900	9350
B	12450	9750
C	11900	9350
D	12950	9350
E	11900	9350
F	11900	10300
G	11900	9350
H	12450	9750
I	11900	9350

TABLE 2

Temp. °C	Symbol	Tensile Stress (psi)	Torsional Stress (psi)	Strain Rate (με/min)	Angle of Normal (deg)
150	G	45000	0	72	0
	F	38000	8100	61	38
	E	33000	12000	69	56
	D	20200	16500	60	64
	C	15100	19200	63	75
	B	6000	19800	73	90⁻
250	G	24500	0	70	0
	E	22500	4500	96	42
	D	16100	7800	68	61
	C	11500	9500	77	78
	B	3500	10800	76	90⁻

TABLE 3

Symbol	Load Path	Tensile Stress (psi)	Torsional Stress (psi)	Angle of Normal (degrees)	Creep Prestrain and Temp.
□	G	47500	0	0	-
	F	39000	9100	54	
	E	29500	14800	62	
	D	21300	15800	68	
	C	14500	17000	83	
	B	6800	20300	90⁻	
	A	1150	22000	90	
X	G	46500	0	0	-
	F	41000	8200	55	
	E	30000	15000	65	
	D	21800	16300	72	
	C	14300	17200	85	
	B	6300	2100	90⁻	
	A	115	21300	90	
+	G	47000	0	0	~500 με
	F	40000	8500	56	250°C
	E	29500	14300	61	
	D	21500	16200	70	
	C	14400	17000	84	
	B	6500	21500	90⁻	
	A	115	22150	90	
Δ	G	46300	0	0	~8000 με
	F	40500	8200	55	250°C
	E	29000	14000	63	
	D	21300	15800	71	
	C	14500	16500	85	
	B	6500	22000	90⁻	
	A	115	21000	90	

(continued)

TABLE 3 (continued)

Symbol	Load Path	Tensile Stress (psi)	Torsional Stress (psi)	Angle of Normal (degrees)	Creep Prestrain and Temp.
O	G	47400	0	0	~8000 με
	F	41000	8200	54	150°C
	E	29300	14500	62	
	D	21300	16500	70	
	C	14200	17000	86	
	B	6500	21800	90	
	A	115	20500	90	

Figure Captions

Fig. 1 Experimental test specimen.

Fig. 2 Variations in primary inelastic equivalent strain rate with time: effect of load path history.

Fig. 3 Variations in the angle of the strain rate vector (arctan $(\dot{\Gamma}/\dot{E})$) with time: effect of load path history.

Fig. 4 Load paths for 250°C secondary creep tests.

Fig. 5 Steady state inelastic equivalent strain rates for the combined stress points of Fig. 4.

Fig. 6 Data points for the low strain rate surface of Fig. 8.

Fig. 7 Variation in equivalent strain rate for the 150°C points of Fig. 6.

Fig. 8 Surfaces of constant steady state inelastic strain rate.

Fig. 9 Normalized initial and subsequent surfaces of constant steady state inelastic strain rate.

Fig. 10 Experimental test points for room temperature yield surfaces.

Fig. 11 Experimental surfaces of constant macro-potential.

Fig. 12 Variations of stress and inelastic strain rate with time for small tensile stress cycle.

Fig. 13 Variations in flow potential for the stress cycle of Fig. 12.

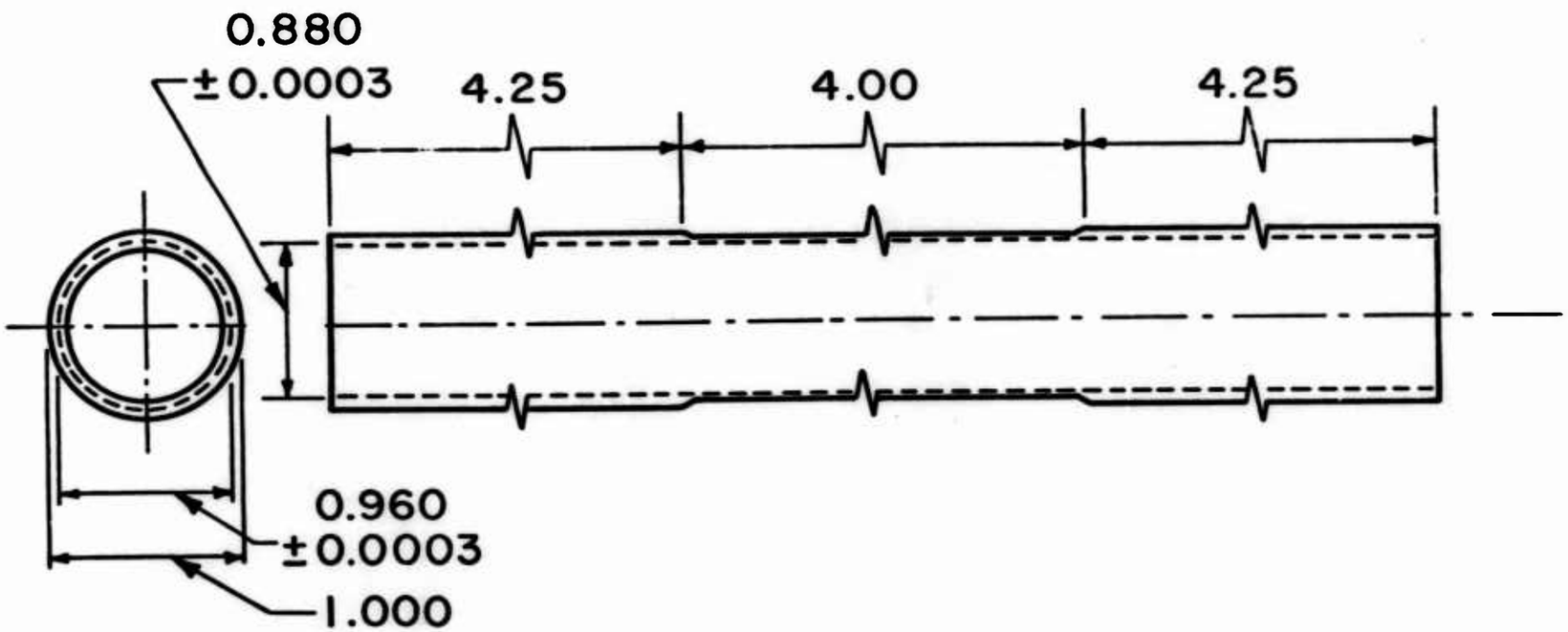

FIGURE 1

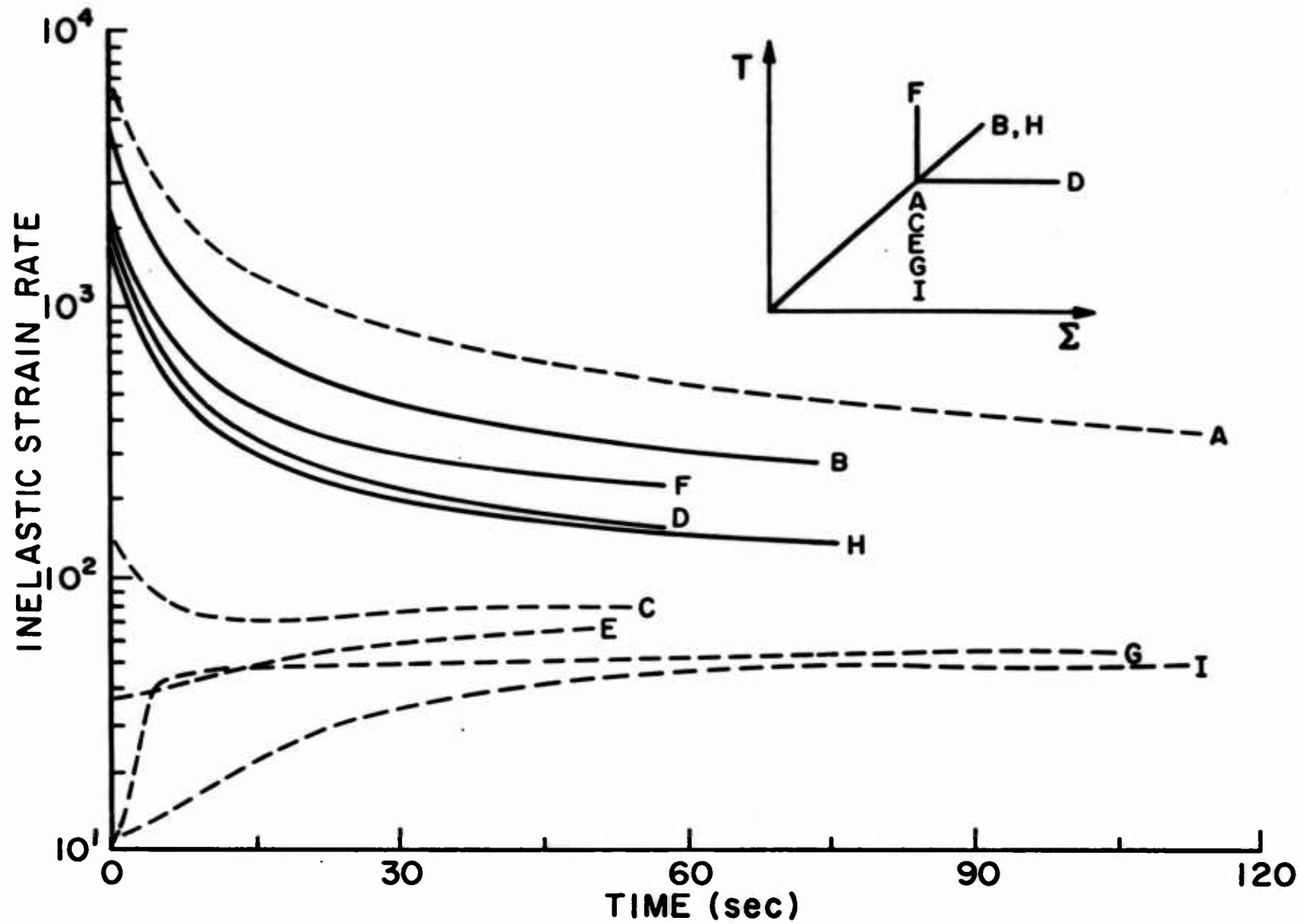
INELASTIC STRAIN RATE
10^4
10^3
10^2
10^1
0
30
60
90
120
TIME (sec)
A
B
C
D
E
F
G
H
I
T
Σ
F
B, H
D
A
C
E
G
I

FIGURE 2

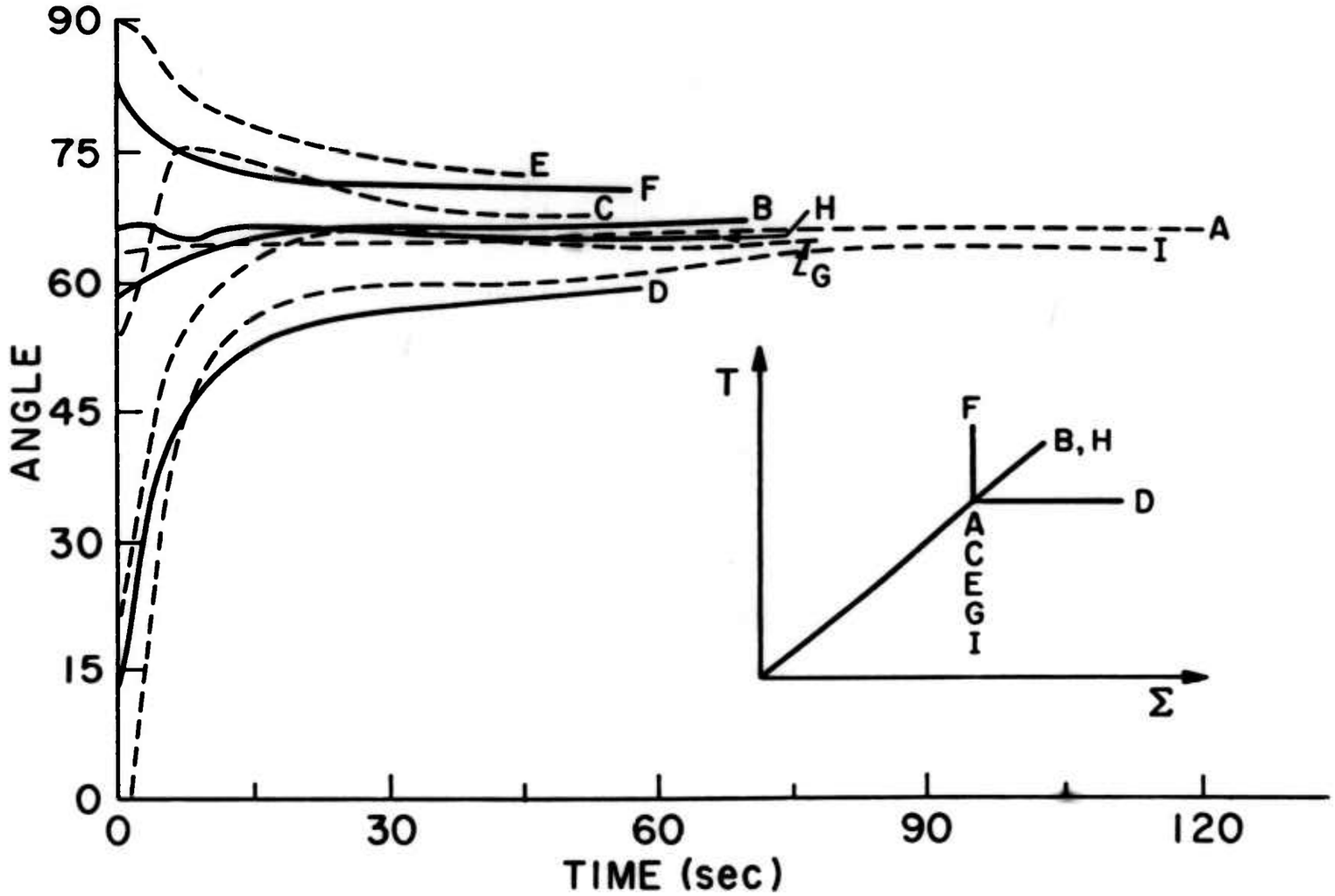
90
75
60
45
30
15
0
ANGLE
0
30
60
90
120
TIME (sec)
E
F
C
B
H
A
I
G
D
T
F
B, H
D
A
C
E
G
I
Σ

FIGURE 3

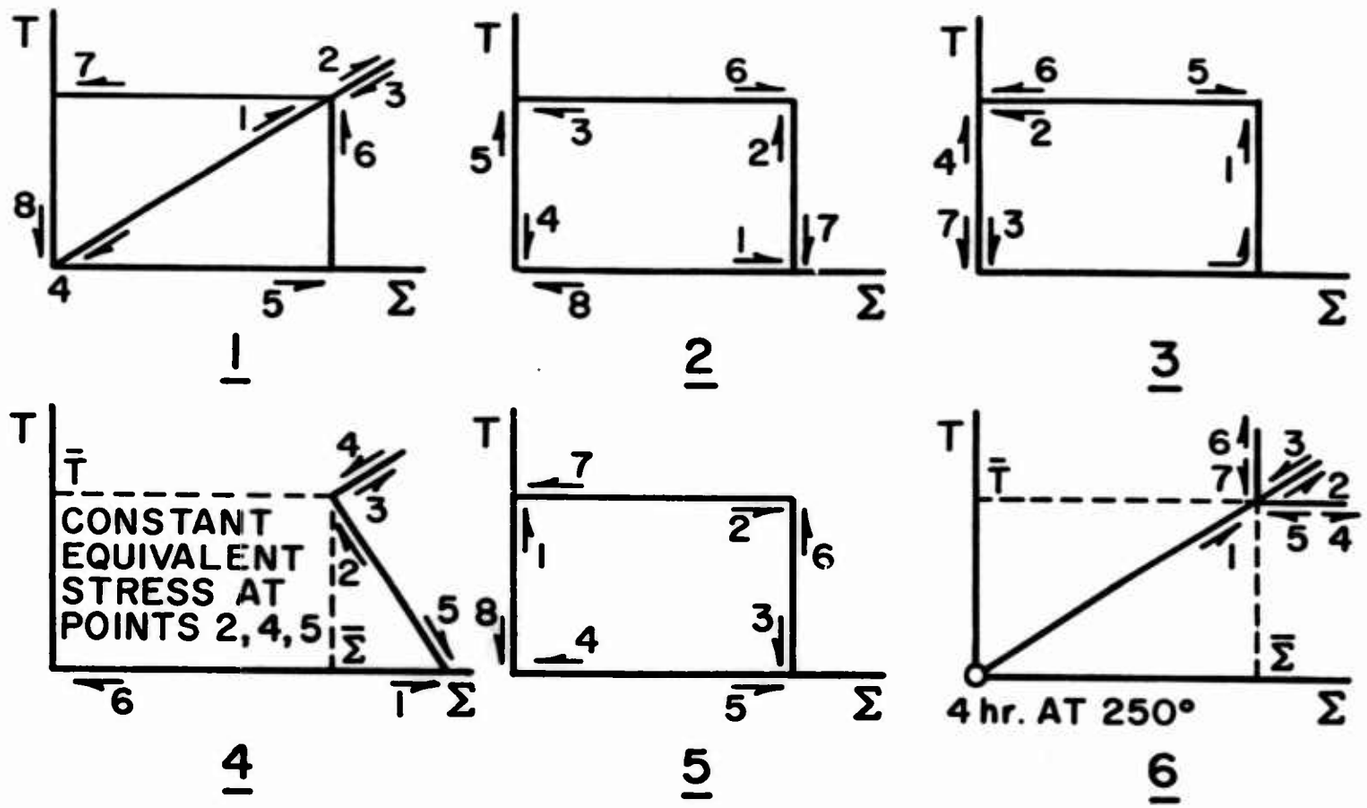

$\bar{\Sigma}$ = 15500 psi
T = 8500 psi

δ(AXIAL LOAD) = 5%
δ(RADIAL LOAD) = 10%

FIGURE 4

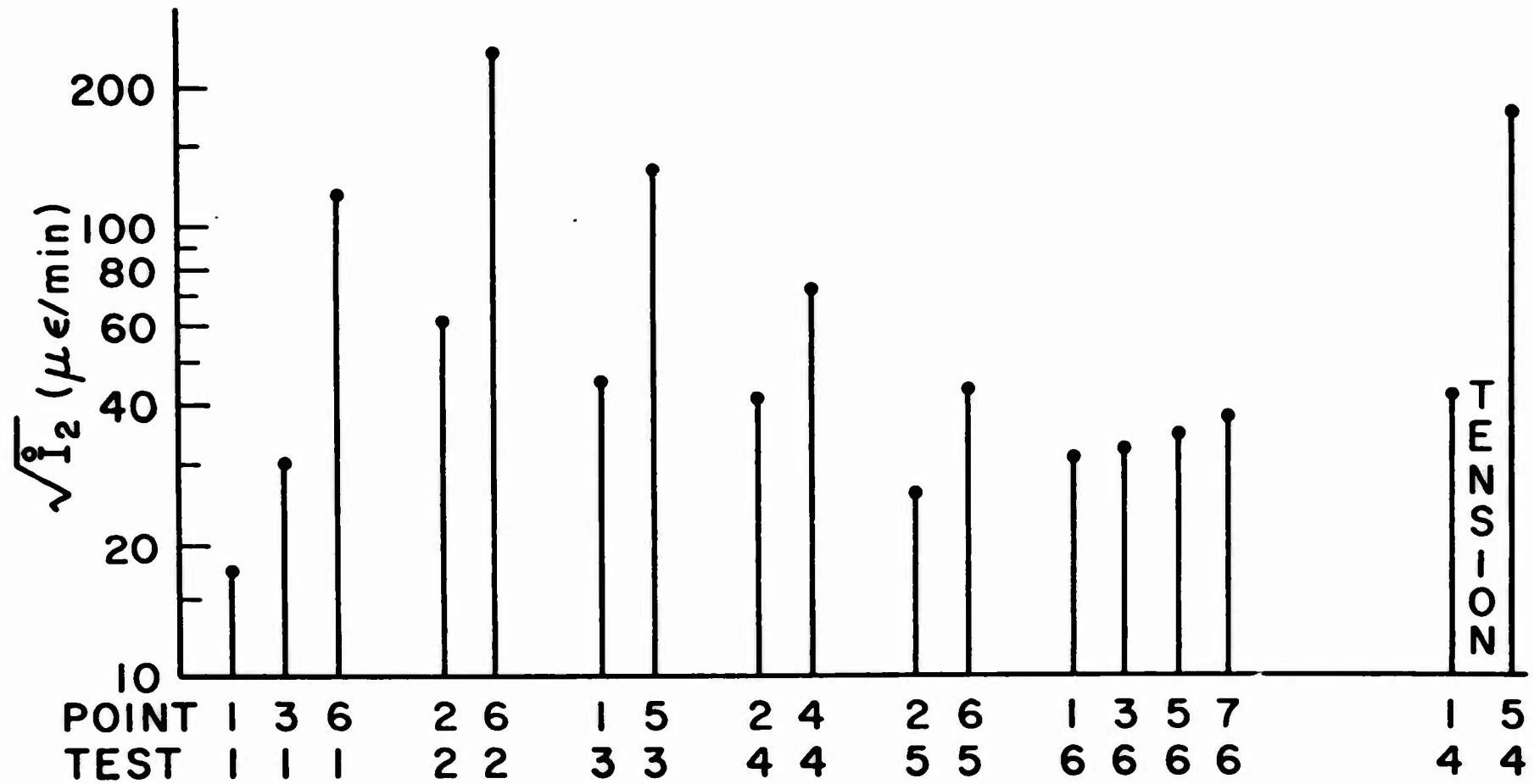
200
100
80
60
40
20
10
$\sqrt{\bar{I}_2}$ ($\mu\epsilon$/min)
TENSION
POINT 1 3 6 2 6 1 5 2 4 2 6 1 3 5 7 1 5
TEST 1 1 1 2 2 3 3 4 4 5 5 6 6 6 6 4 4

FIGURE 5

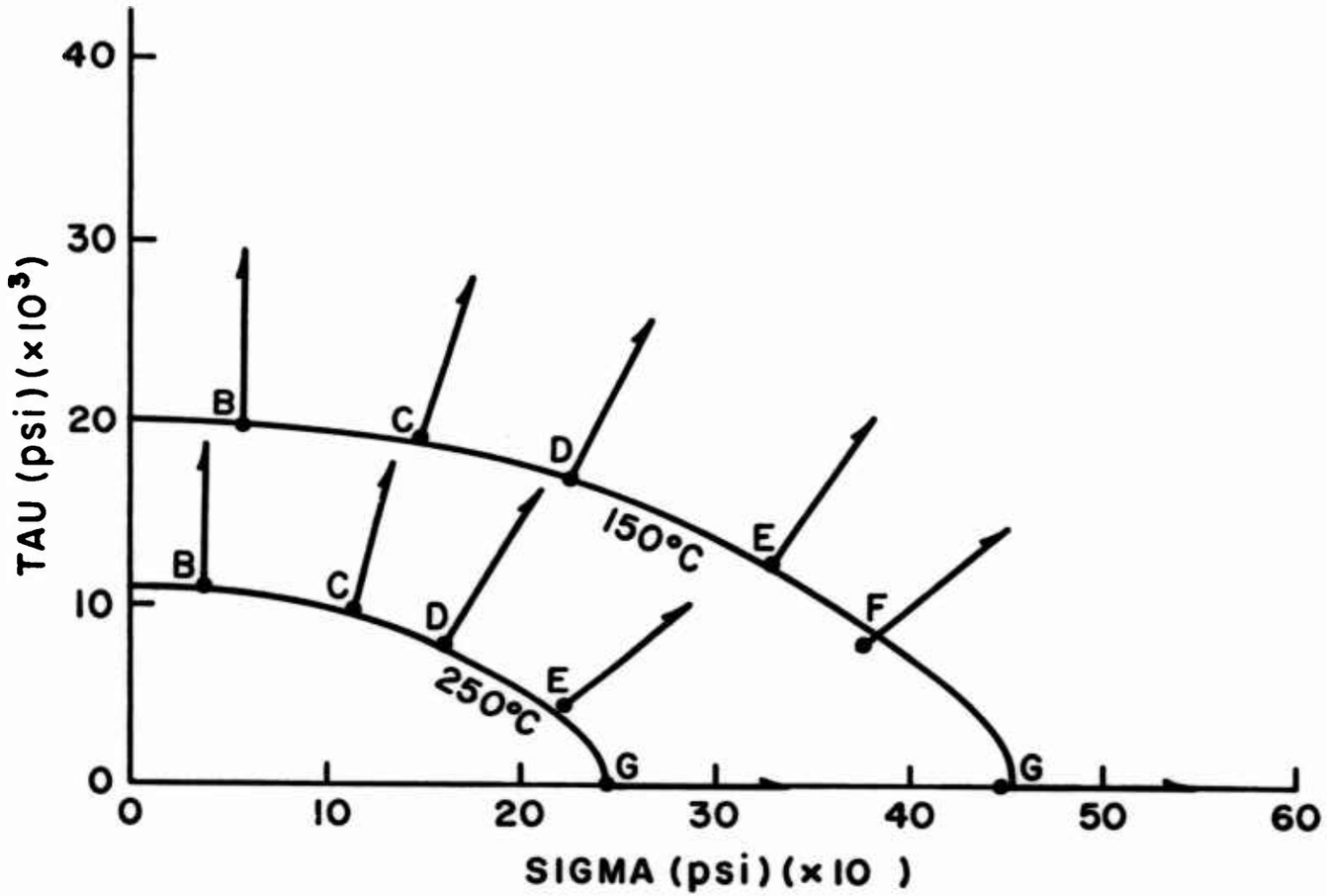
40
30
20
10
0
TAU (psi) (x10³)
B
C
D
E
F
G
150°C
250°C
0
10
20
30
40
50
60
SIGMA (psi) (x10)

FIGURE 6

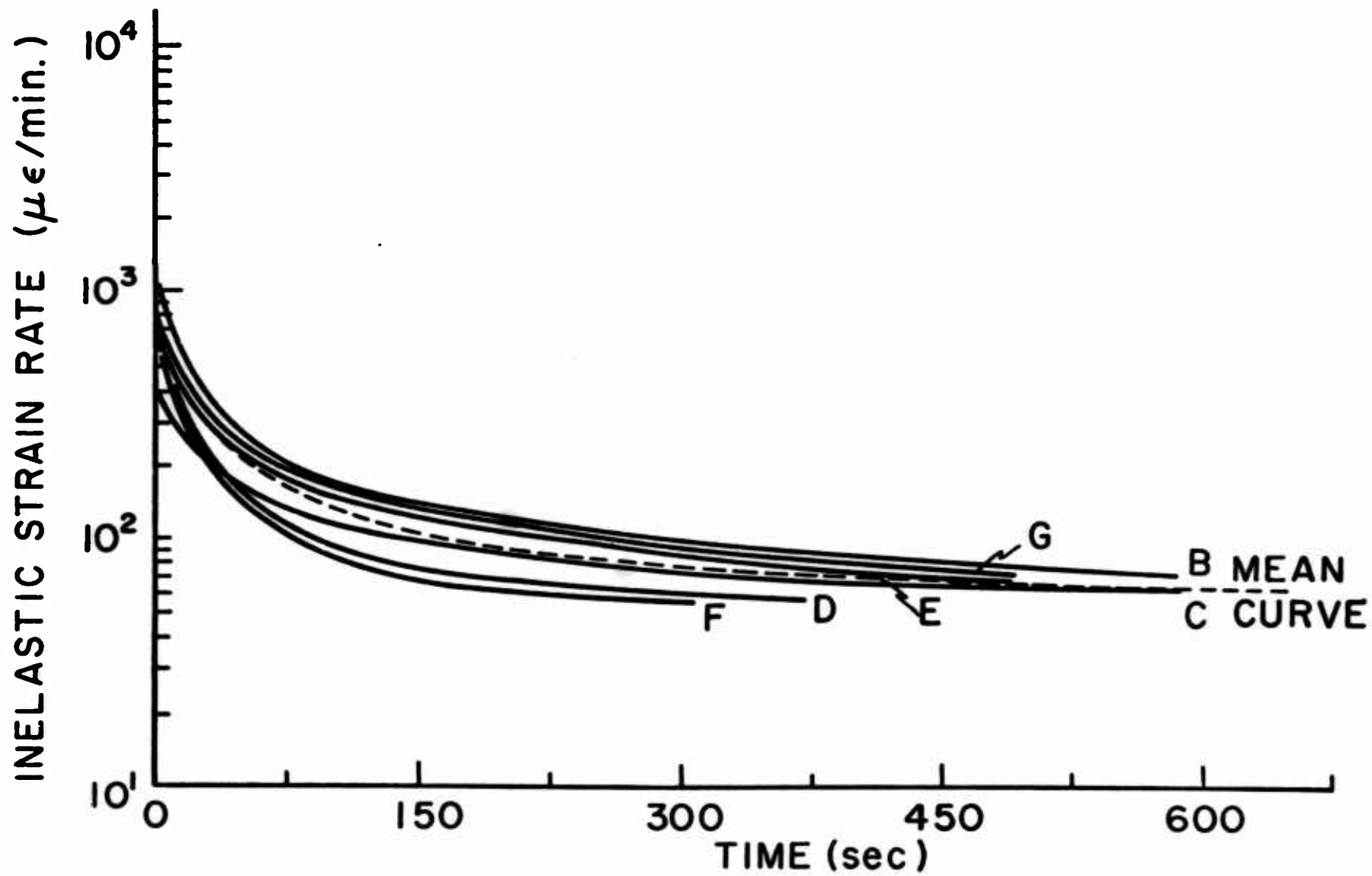
INELASTIC STRAIN RATE (με/min.)
10⁴
10³
10²
10¹
0
150
300
450
600
TIME (sec)
G
B
MEAN
C
CURVE
F
D
E

FIGURE 7

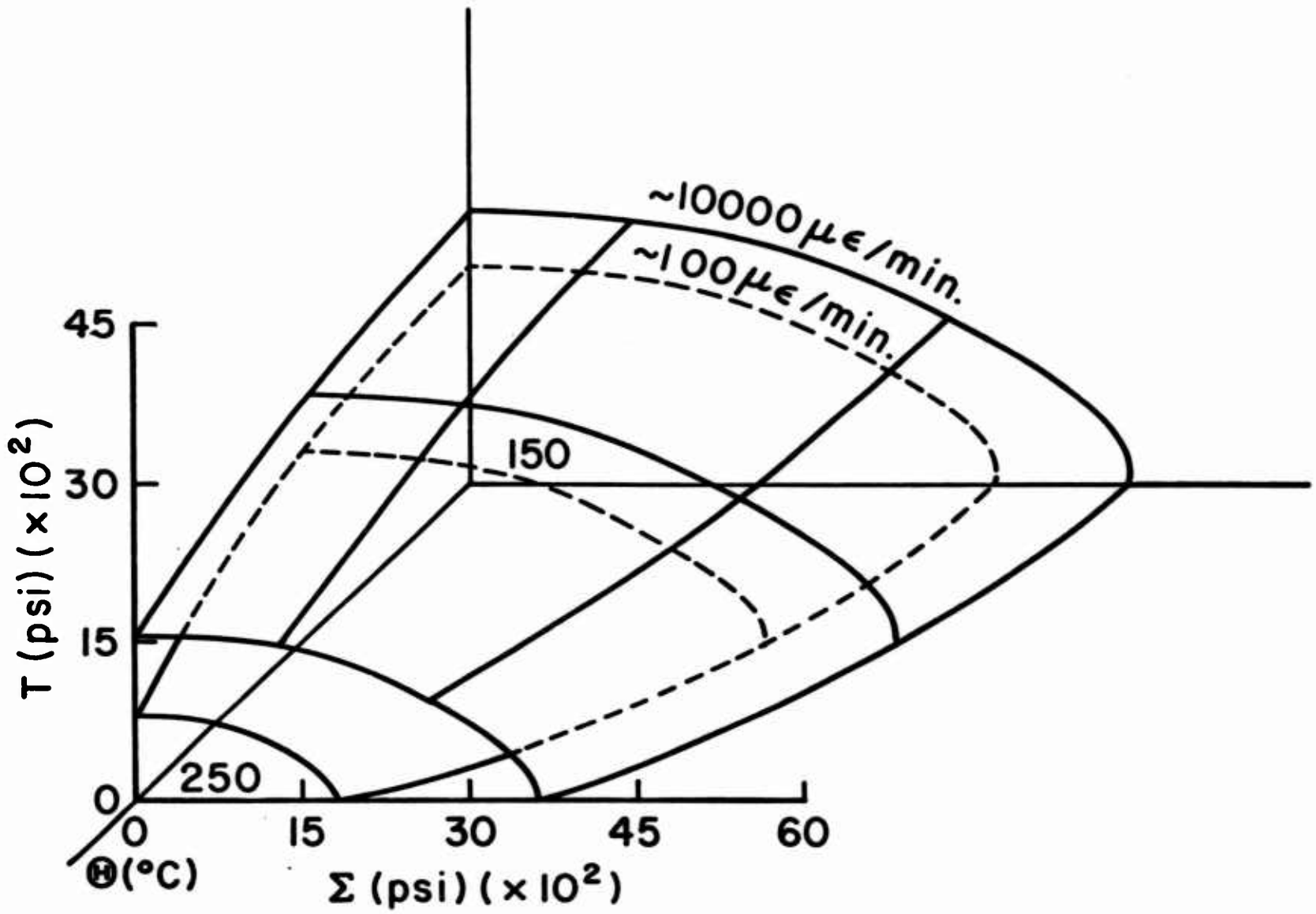
~10000 με/min.
~100 με/min.
150
250
45
30
15
0
T (psi) (× 10²)
0
15
30
45
60
Θ(°C)
Σ (psi) (× 10²)

FIGURE 8

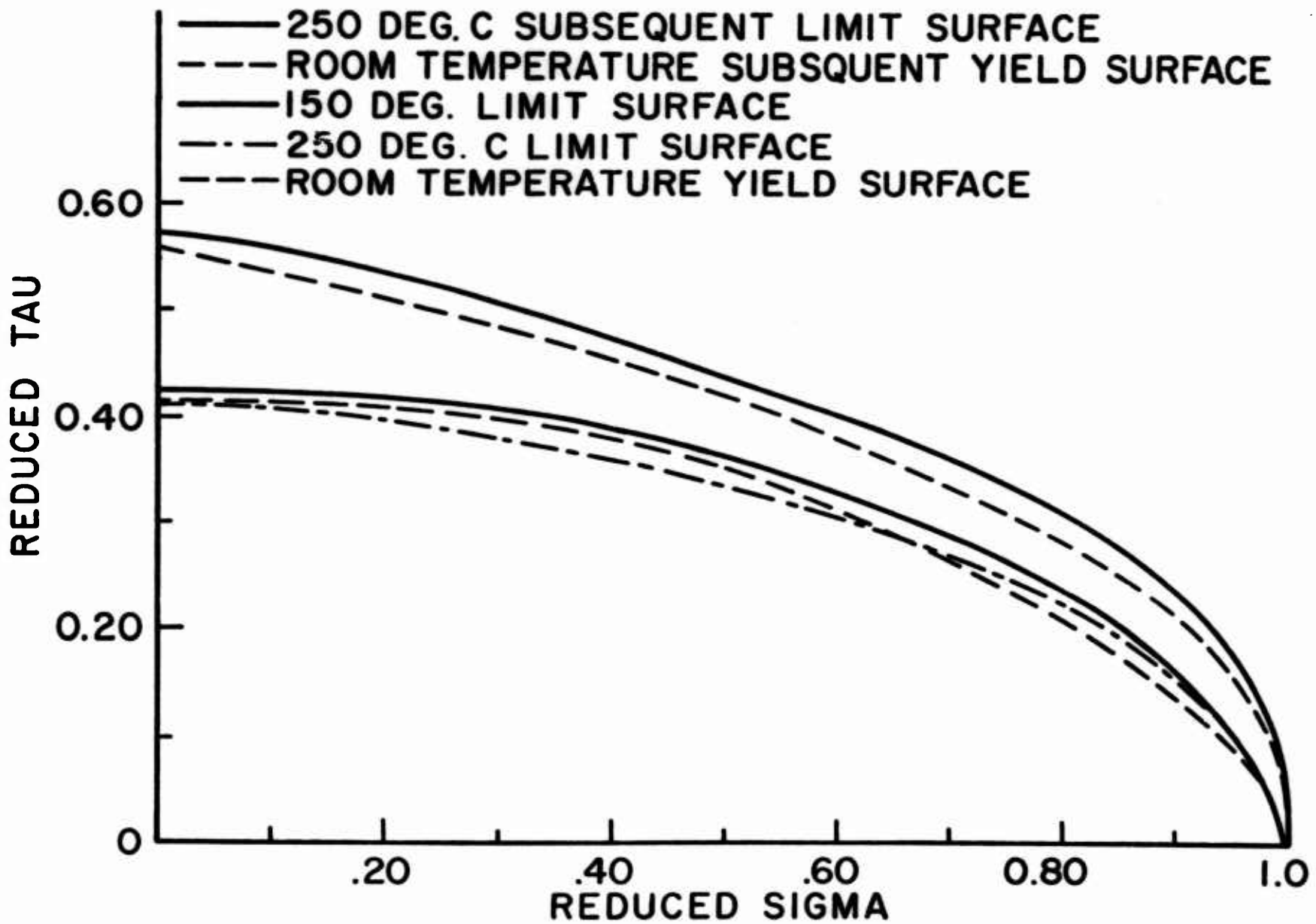
250 DEG. C SUBSEQUENT LIMIT SURFACE
ROOM TEMPERATURE SUBSQUENT YIELD SURFACE
150 DEG. LIMIT SURFACE
250 DEG. C LIMIT SURFACE
ROOM TEMPERATURE YIELD SURFACE
REDUCED TAU
0.60
0.40
0.20
0
.20
.40
.60
0.80
1.0
REDUCED SIGMA

FIGURE 9

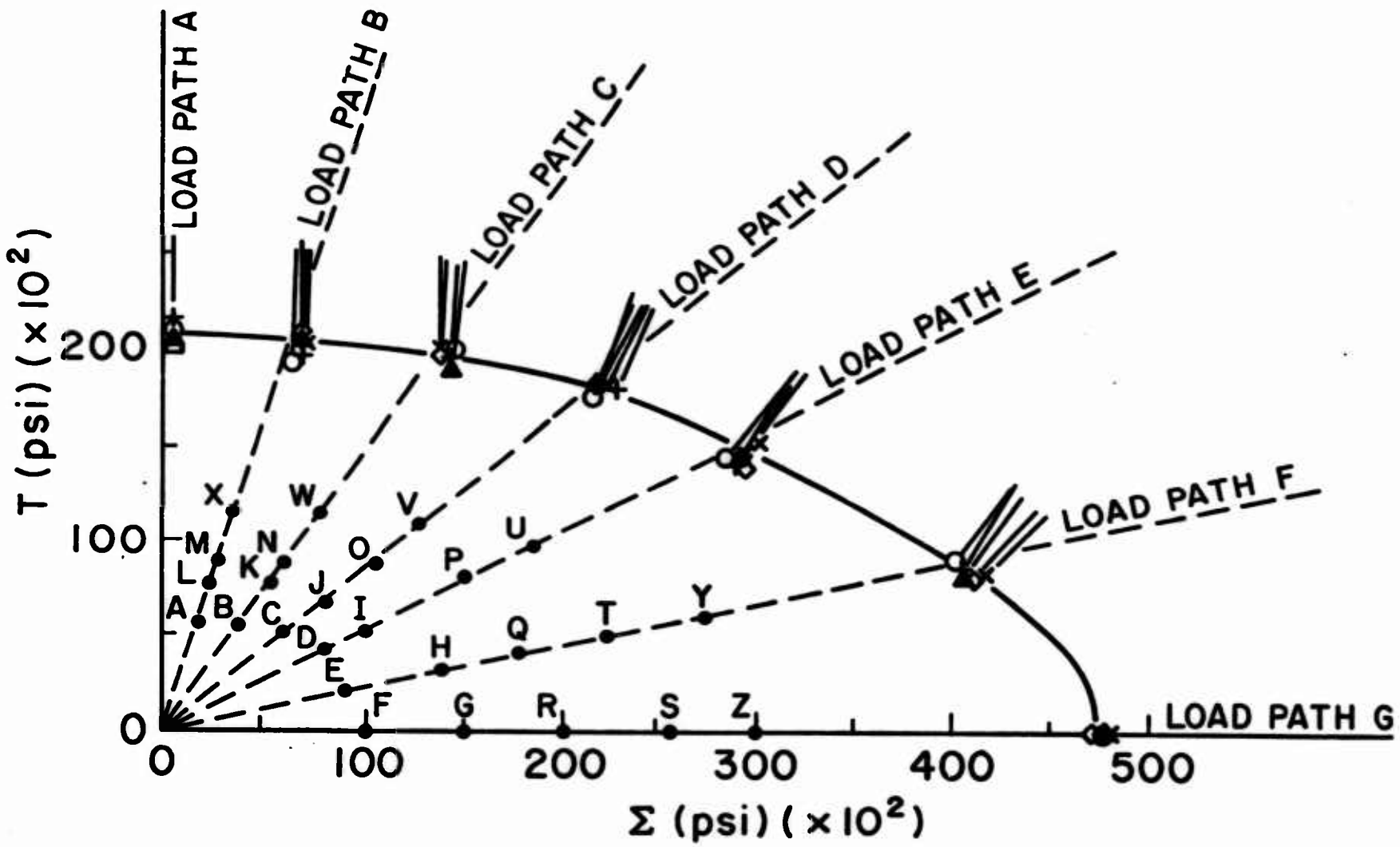
LOAD PATH A
LOAD PATH B
LOAD PATH C
LOAD PATH D
LOAD PATH E
LOAD PATH F
LOAD PATH G
T (psi) (×10²)
Σ (psi) (×10²)
0
100
200
300
400
500
A
B
C
D
E
F
G
H
I
J
K
L
M
N
O
P
Q
R
S
T
U
V
W
X
Y
Z

FIGURE 10

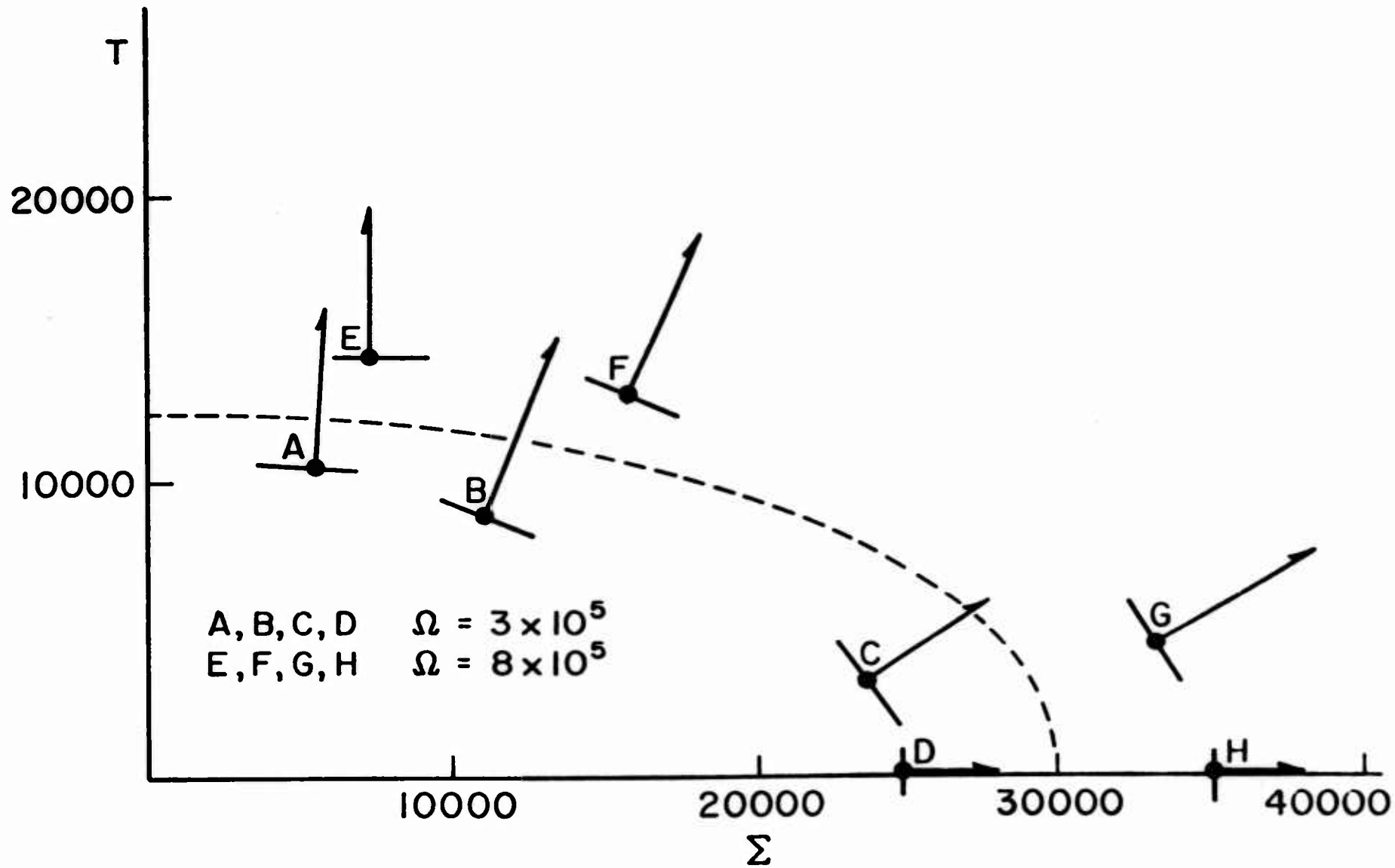
T
20000
10000
E
A
B
F
C
G
D
H
A, B, C, D Ω = 3 × 10^5
E, F, G, H Ω = 8 × 10^5
10000
20000
30000
40000
Σ

FIGURE 11

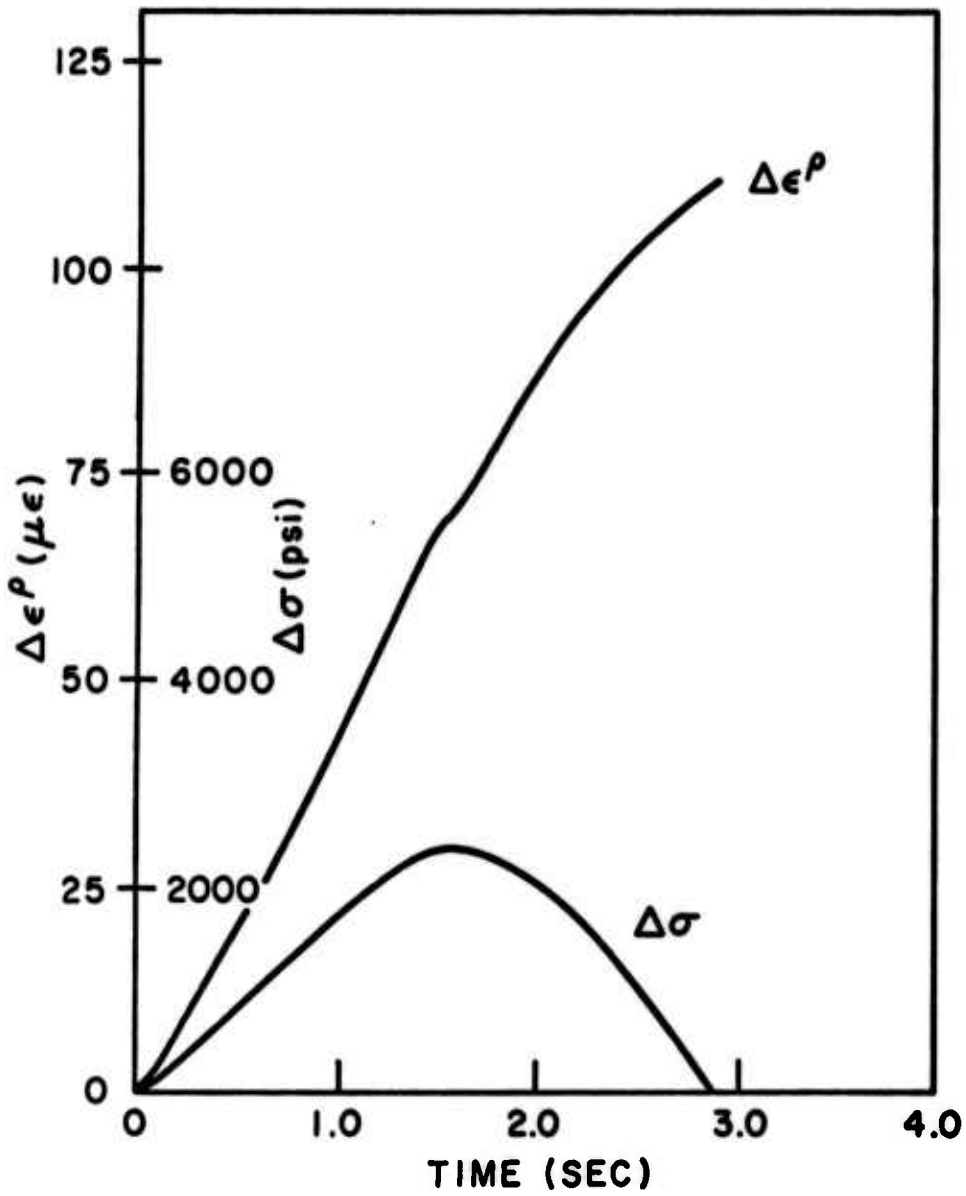
125
100
75
50
25
0
6000
4000
2000
$\Delta\epsilon^p$ ($\mu\epsilon$)
$\Delta\sigma$ (psi)
$\Delta\epsilon^p$
$\Delta\sigma$
0
1.0
2.0
3.0
4.0
TIME (SEC)

FIGURE 12

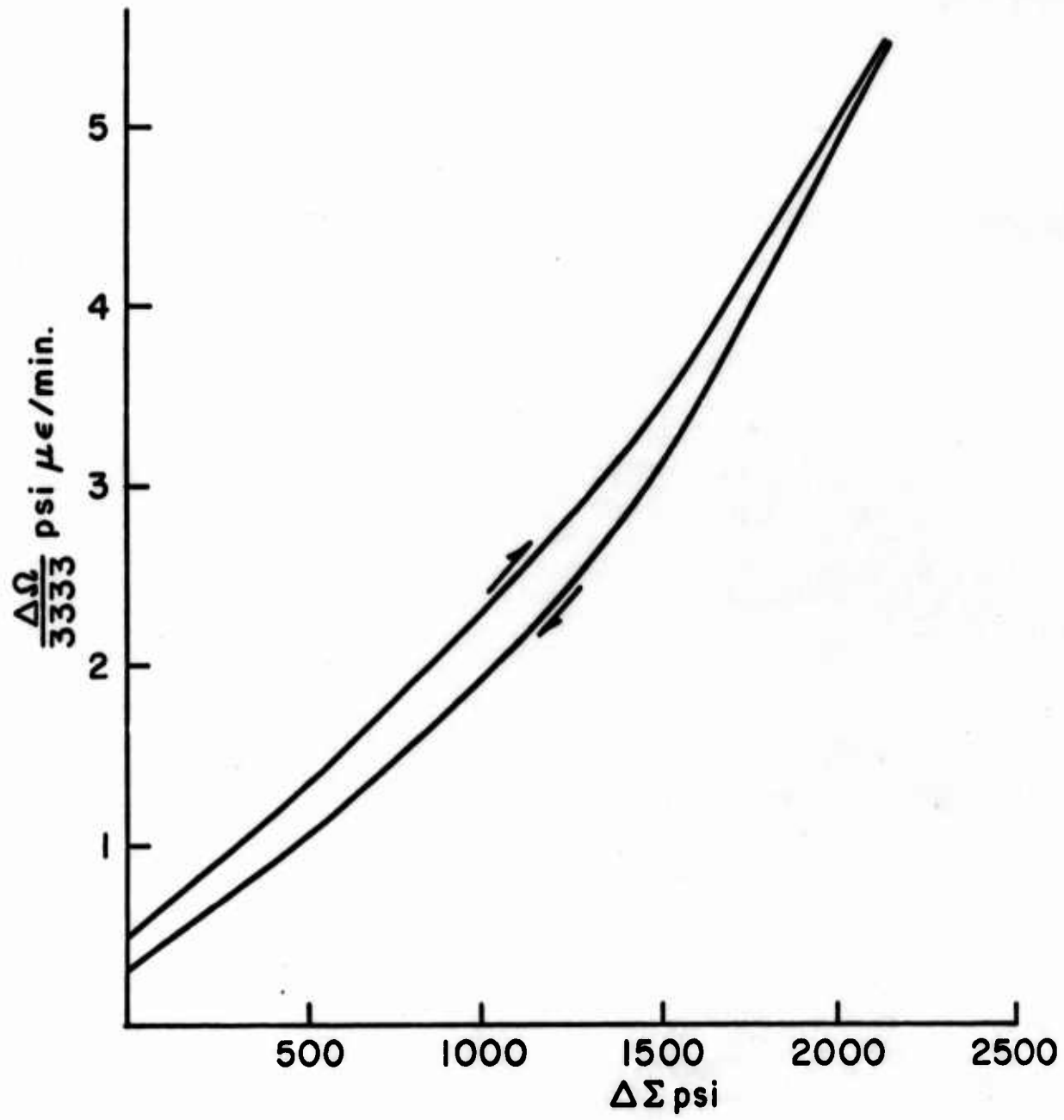
5
4
3
2
1
$\frac{\Delta\Omega}{3333}$ psi $\mu\epsilon$/min.
500
1000
1500
2000
2500
$\Delta\Sigma$ psi

FIGURE 13

Security Classification

DOCUMENT CONTROL DATA - R & D

(Security classification of title, body of abstract and indexing annotation must be entered when the overall report is classified)

1. ORIGINATING ACTIVITY *(Corporate author)* Brown University, Engineering Division Providence, Rhode Island	2a. REPORT SECURITY CLASSIFICATION Unclassified 2b. GROUP

3. REPORT TITLE

Inelastic Deformation of an Aluminum Alloy Under Combined Stress at Elevated Temperature

4. DESCRIPTIVE NOTES *(Type of report and inclusive dates)*

Technical Report

5. AUTHOR(S) *(First name, middle initial, last name)*

G. M. Brown

6. REPORT DATE July 1970	7a. TOTAL NO. OF PAGES 32	7b. NO. OF REFS 12
8a. CONTRACT OR GRANT NO. N00014-67-A-0191-0003 b. PROJECT NO. c. TASK NR 064-424 d.	9a. ORIGINATOR'S REPORT NUMBER(S) N00014-67-A-0191-0003/10 9b. OTHER REPORT NO(S) *(Any other numbers that may be assigned this report)*	

10. DISTRIBUTION STATEMENT

11. SUPPLEMENTARY NOTES	12. SPONSORING MILITARY ACTIVITY Office of Naval Research Boston Branch Office, 495 Summer Street Boston 10, Massachusetts

13. ABSTRACT

Biaxial stress tests were performed on thin wall tubes of polycrystalline 2024-T81 Aluminum at temperatures of 150 and 250°c. The nominal metallurgical stabilization temperature for this alloy is 190°c. Transient and steady state creep strain rates exhibited a considerable dependence on load path history. For a prescribed history it is possible to determine unique surfaces of constant creep strain rate. For the zero history, involving a single loading from the origin to a prescribed point in stress space, surfaces of constant steady state strain rate, at elevated temperature, have the same shape as room temperature yield surfaces of moderate offset. In the temperature and small strain regions considered here, room temperature yield surfaces were found to be unaffected by elevated temperature deformation. The changes in shape of room temperature yield surfaces, due to room temperature plastic deformation caused corresponding changes in the elevated temperature surfaces of constant steady state creep rate. At a given stress point, an outward local motion of the yield surface resulted in a corresponding outward local motion of the steady state creep rate surfaces. The experimental determination of surfaces of constant flow potential was also attempted.

DD FORM 1 NOV 65 1473

Security Classification

Security Classification

14. KEY WORDS	LINK A ROLE	LINK A WT	LINK B ROLE	LINK B WT	LINK C ROLE	LINK C WT
experimental						
creep						
yield						
surface						
temperature						
history						
flow potential						

Security Classification